Original Article

Clin Shoulder Elbow 2024;27(3):272-277
https://doi.org/10.5397/cise.2023.01165

CiSE
Clinics in Shoulder and Elbow

eISSN 2288-8721

Surgical anatomical landmarks for arthroscopic repair of subscapularis tendon tears

Santiago Gabardo, María Valencia-Mora, Ismael Coifman, Emilio Calvo

Shoulder and Elbow Reconstructive Surgery Unit, Department of Orthopedic Surgery and Traumatology, Hospital Universitario Fundación Jiménez Díaz, Universidad Autónoma de Madrid, Madrid, Spain

Background: Subscapularis repair has recently garnered significant interest. A thorough understanding of the tendon's anatomy is essential for precise and safe repair. Our objectives were to describe the anatomy of the subscapularis insertion, define its landmarks, and analyze nearby structures to guide arthroscopic repair.
Methods: We conducted an anatomical study, dissecting 12 shoulders. We evaluated the distance from the footprint to the axillary nerve, the dimensions, and shape of the footprint, and its relationship with the humeral cartilage.
Results: The distance to the axillary nerve was 32 mm (standard deviation [SD], 3.7 mm). The craniocaudal length of the footprint was 37.3 mm (SD, 4.6 mm). Its largest mediolateral thickness was 16 mm (SD, 2.2 mm), wider at the top and narrower distally. The distance between the footprint and the cartilage varied, being 3.2 mm (SD, 1.2 mm) in the upper part, 5.4 mm (SD, 1.8 mm) in the medium, and 15.9 mm (SD, 2.9 mm) in the lower part.
Conclusions: When performing a repair of the subscapularis tendon, the distance to the cartilage should be carefully evaluated as it varies proximally to distally, and the shape of the footprint (wider proximally, tapered distally) should be considered for implant positioning. The distance to the axillary nerve is approximately 30 mm. Anterior visualization guarantees direct control of all landmarks and allows accurate implant positioning with safe tendon release.
Level of evidence: IV.

Keywords: Rotator cuff injuries; Subscapularis; Arthroscopy; Rotator cuff tears

INTRODUCTION

The subscapularis (SSC) is the most powerful muscle of the rotator cuff. The SCC is not only an essential internal rotator of the shoulder, but it is also involved in stabilizing the glenohumeral joint and impacts the optimal function of the long head of the biceps [1]. The incidence of SSC tears is lower than that of posterosuperior rotator cuff tears, and less attention has been placed on the SCC anatomy [1]. To achieve accurate and safe repair of SSC tears, a thorough understanding of the SSC insertion anatomy is required, including the shape, location, and surrounding structures.

While open and arthroscopic techniques are used to repair the SSC [2], the arthroscopic approach is more common. However, arthroscopic repair of SSC is incredibly challenging. The full extent of the tendon can be difficult to visualize due to its close proximity with the glenohumeral capsule and neurovascular structures, highlighting the importance of tendon and muscular releases. Furthermore, the SSC footprint is adjacent to the hu-

Received: December 30, 2023 Revised: February 18, 2024 Accepted: March 2, 2024
Correspondence to: Santiago Gabardo
Shoulder and Elbow Reconstructive Surgery Unit, Department of Orthopedic Surgery and Traumatology, Hospital Universitario Fundación Jiménez Díaz, Universidad Autónoma de Madrid, Av. de los Reyes Católicos, 2, 28040, Madrid, Spain
Tel: +34-6-1626-6064, E-mail: gabardosantiago@gmail.com, ORCID: https://orcid.org/0000-0001-9242-8634

meral articular cartilage that might be invaded during anchor insertion. Various arthroscopic approaches have been proposed to overcome these challenges using either a conventional posterior portal or an anterolateral portal for visualization [3-5]. There is controversy on the best way to approach SSC tendon repair. Many surgeons advocate for a posterior view with the scope inserted into the glenohumeral joint, while other surgeons prefer to visualize the tendon from the front [6]. This study aims to describe the anatomy of the SSC tendon insertion, to define its landmarks and the distances to nearby structures that might potentially be at risk, and to serve as a guide for safe repair.

METHODS

We conducted an anatomical study with cadaveric dissection. As the study was a cadaveric research, conducted on cadavers donated to our university, the requirement for approval of the institutional review board was exempted. This study included 12 shoulders from 6 cadavers preserved with the standardized Thiel embalming method. Relevant anatomical landmarks for SSC repair were studied, including the relationships of the footprint with the axillary nerve and the bicipital grove, the dimensions and shape of the footprint, and the distance from the medial margin of the footprint to the humeral head cartilage.

A standard deltopectoral approach was performed in all cadavers, and the deltopectoral fascia was opened longitudinally. The space between the deltoid and the pectoralis major muscles was opened using blunt dissection, the clavipectoral fascia below was incised using a scalpel, and the deltoid muscle was retracted laterally. The coracoid process was osteotomized to retract the conjoint tendon medially, permitting easy identification and access to the bicipital groove, the SSC tendon insertion, and the anterior aspect of the muscle. The distance was measured from the most inferior edge of the SSC insertion to the vertically closest point of the axillary nerve in mm. Next, we evaluated the bicipital groove and its relation to the SSC tendon insertion. The transverse and coracohumeral ligaments and the synovial sheath of the long head of the biceps tendon were opened; the tendon was detached from its upper insertion on the glenoid tubercle and removed distal to the lesser tuberosity. Finally, the insertion of the SSC was peeled from lateral to medial and from superior to inferior to obtain a precise view of the SSC footprint and to evaluate the anatomic relations between the articular aspect of the tendon and the glenohumeral capsule. The size of the footprint was measured. The length was measured from the upper limit of the footprint to the most inferior muscular insertion of the SSC. The width was measured from medial to lateral at the widest area of the footprint. The distance from the SSC insertion to the lateral edge of the humeral head cartilage was measured at three levels: (1) superior, at the uppermost edge of the footprint; (2) intermediate or medium, at a level equidistant to the upper edge and to the most inferior limit of the footprint; and (3) inferior, at the most inferior limit of the footprint corresponding to the tendinous insertion of the SSC (Fig. 1). The possibility of differentiating the SSC tendon and the capsule was assessed across the footprint in each specimen. The distance from the muscular insertion of the SSC to the humeral head cartilage was not considered since it is not usually reconstructed when the SSC tendon is repaired. All measurements were systematically obtained with cadavers in supine position and the shoulders in neutral rotation,

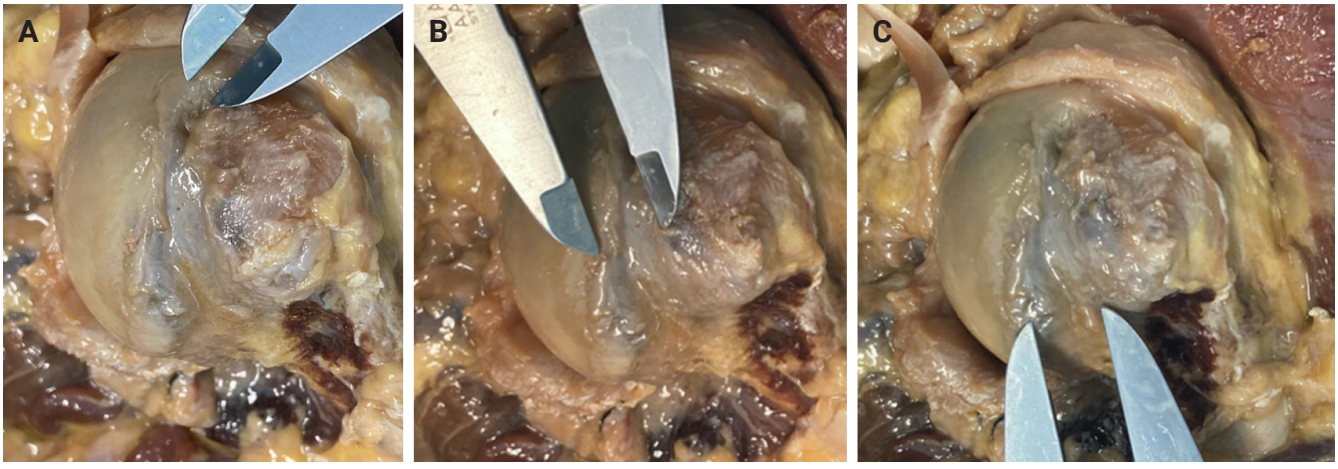

Fig. 1. Close front view of the left shoulder after deltoid approach and subscapularis (SSC) insertion detachment. Representative measurement of the distance from the footprint to the cartilage, superior (A), medial (B) and inferior (C). The full SSC insertion at the humerus, the tendinous part covering the greater tuberosity, and an underlying muscular insertion.

0º abduction, and 90º elbow flexion. A vernier caliper (Aesculap, B. Braun) was used for measurements [7]. Mean and standard deviation were used to describe quantitative variables, and frequency and percentage were used for qualitative variables, assuming a normal distribution of values.

RESULTS

This study analyzed six cadavers (four female and two male). The average height was 162.5 cm and the average weight was 65 kg. All shoulders showed intact SSC and long head of biceps anatomy. The mean safety distance from the bottom tip of the footprint to the axillar nerve was 32 mm (standard deviation [SD], 3.7), with a range of 25–35 mm. After removal of the long head of the biceps and dissection of its groove, a soft tissue layer that extended from the deepest fibers of the SSC tendon to cover the floor of the upper portion of the bicipital groove was encountered in nine shoulders (Fig. 2).

The upper tendinous and lower muscular portions were easily identified in all specimens by detaching the SSC from its footprint. The tendinous portion was attached to the lesser tuberosity while the muscular portion extended inferiorly to the humeral neck. The footprint of the SSC was wider proximally and became progressively narrower distally (Fig. 3). The mean footprint length from cranial to caudal was 37.3 mm (SD, 4.6 mm), and the mean width measured at the broadest portion was 16 mm (SD, 2.2 mm). The mean distance from the footprint to the humeral head cartilage was 3.2 mm (SD, 1.2 mm) superiorly, 5.4 mm (SD, 1.8 mm) in the medium part, and 15.9 mm (SD, 2.9 mm) inferiorly (Fig. 3). The joint capsule was closely integrated into the tendinous portion at the tendon insertion and could only be individualized in one case (Fig. 4).

DISCUSSION

This study had several important findings. First, there is a mini-

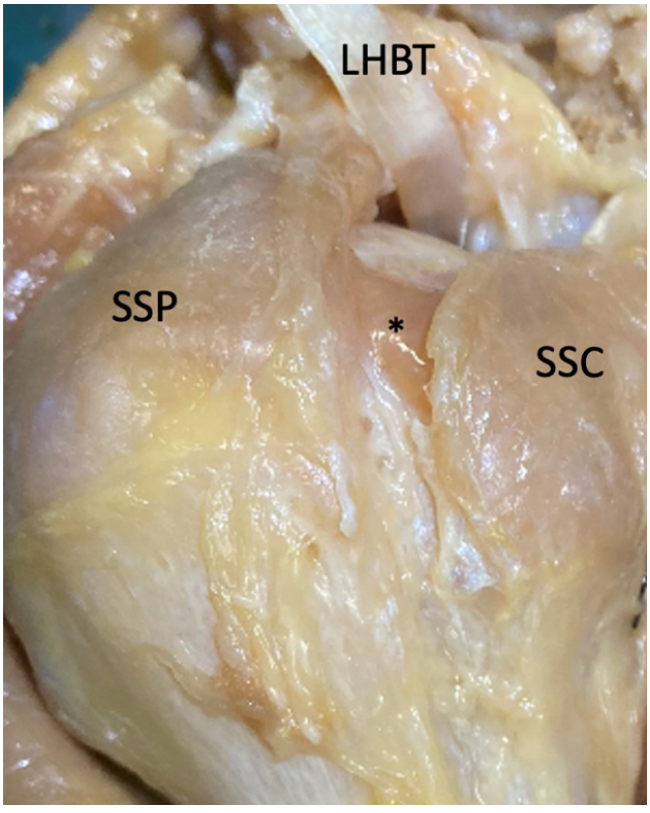

Fig. 2. Lateral view of the right shoulder after the deltoid approach, bursa resection, and distal long head of the biceps tendon (LHBT) dissection and retraction. The image shows the floor of the bicipital groove, where soft tissue is dependent on the subscapularis (SSC). SSP: supraspinatus insertion. Asterisk: soft tissue dependent on the SSC.

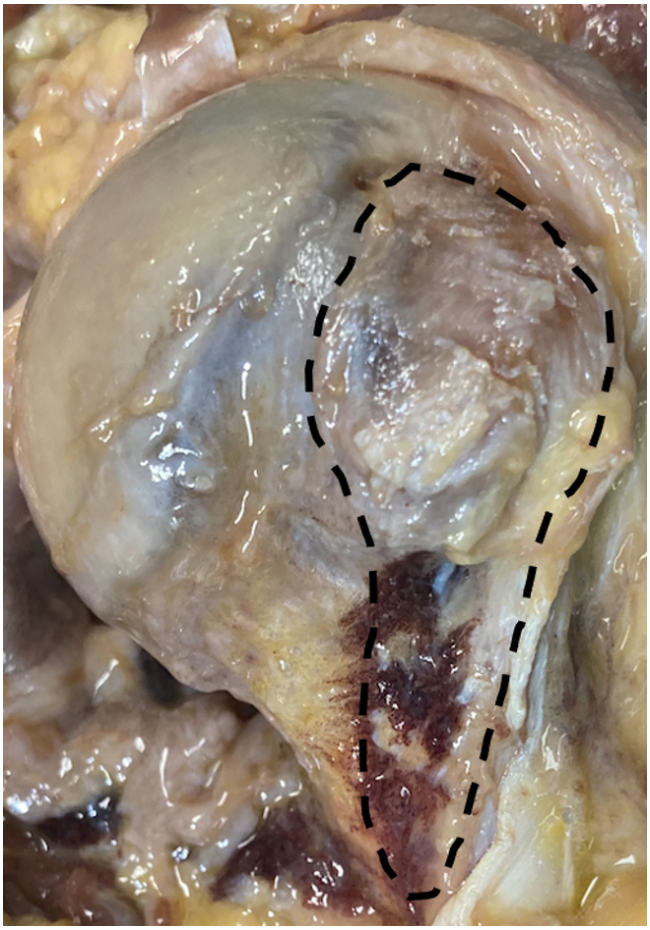

Fig. 3. Subscapular footprint after peeling of the tendon viewed from the anterior aspect. Dashed line: outline of the subscapular footprint, including both the tendinous and muscular portions.

https://doi.org/10.5397/cise.2023.01165

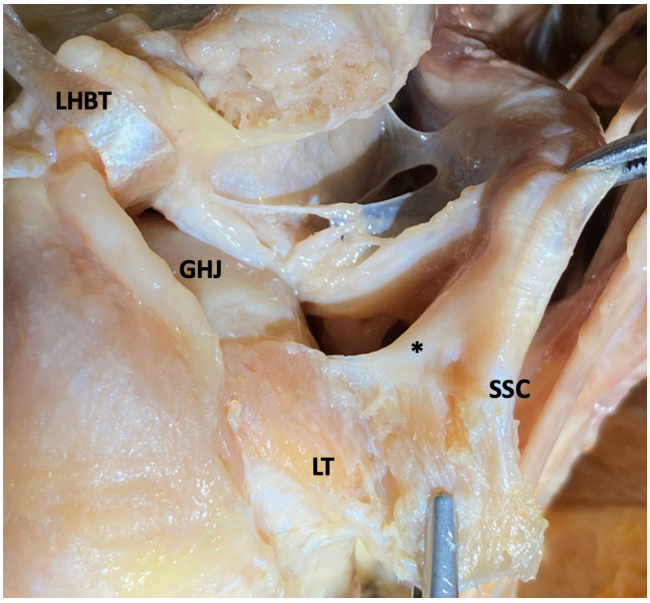

Fig. 4. Lateral view of the right shoulder after deltoid approach, bursa resection, and partial insertion detachment. The image shows the surrounding subscapularis (SSC) insertion structures and the close relationship between the SSC tendon and the joint capsule. LHBT: long head of the biceps tendon, GHJ: glenohumeral joint, LT; lesser tubercle. Asterisk: joint capsule.

mum 2.5 cm safe working area between the lower limit of the SSC footprint and the axillary nerve. Second, the most superior part of the SSC tendon extends under the biceps tendon to form the fibrocartilaginous floor of the bicipital groove (Fig. 2). Third, the SSC footprint is broad proximally and tapered distally at the muscular insertion (Fig. 3). Fourth, there is an identifiable stripe of bare bone between the tendon insertion and the humeral head cartilage that becomes wider inferiorly (Fig. 1). Fifth, SSC is closely united to the glenohumeral capsule along its insertion (Fig. 4).

The axillary nerve runs anterior to the SSC and branches to innervate its most inferolateral region before exiting through the quadrilateral space [8]. For open and arthroscopic surgeries, it is essential to know that the axillar nerve runs below the SSC tendon, being even closer in women and thin patients and with shoulder abduction and internal rotation [9]. We found a mean distance of 3.2 cm from the axillary nerve to the SSC footprint, consistent with previous reports [7] and confirming that there is enough room to carry out a safe repair with minimal risk of nerve damage when reattaching the inferior fibers of the tendon. In retracted SSC tears, 3 cm should be considered the safe medial limit to release the tendon without putting the axillary nerve at risk. However, axillary nerve visualization is strongly recommended when repairing retracted SSC tears.

The SSC tendon forms the medial pulley of the long head of the biceps. We observed a soft tissue structure at the uppermost region of the floor of the bicipital groove that appeared to represent a clear continuation of the SSC when dissected. Clark and Harryman [10] were the first to report that the topmost part of the SSC tendon passes beneath the biceps tendon to create the fibrocartilaginous base of the bicipital groove. Previous studies have identified this tissue has been previously identified as a flap of the SSC tendon and part of the medial pulley [11,12]. The function attributed to this flap is to prevent medial subluxation of the biceps tendon; therefore, it may play a critical role in both the initiation and progression of SSC tears. When the SSC tendon is torn, the medial biceps pulley is also disrupted. Accordingly, the most superior fibers of the tendon must be anatomically reattached to this original site to reconstruct the medial pulley. While the long head of the biceps medial pulley can be comfortably restored in acute tears, reconstruction is not possible in most chronic lesions, and a biceps tenodesis or tenotomy is recommended. The continuity between this soft tissue layer covering the bicipital groove and the SSC tendon may play a critical role in the development of intratendinous SSC tears. This type of tear occurs with an intact biceps pulley and rotator interval. Diagnosing this type of tear using arthroscopy can be challenging because the tendon's articular and bursal sides are preserved [13].

Several previous articles have described the shape of the SSC footprint as ear-shaped [14], trapezoid-shaped [15], or comma-shaped [16]. Its insertion in the wider upper area is tendinous, while that in the narrow and lower region is muscular [16,17]. Regarding dimensions, some studies only measured the tendinous insertion of the SSC, approximately 25 mm in length [15], while other studies also measured the muscular insertion, estimating an average of 40 mm [14]. This study also shows that the SSC insertion is broad proximally and tapered distally (Fig. 3). Double row repair is recommended in the superior two-thirds of the tendon, at the widest point of the footprint, while single-row repair seems preferable in the inferior third.

Some studies stated that there was no space from the lateral margin of the footprint to the cartilage, especially in its upper area [18]. More recent studies showed the presence of bare space between the cartilage and the SSC attachment [16]. Our study found that, although small, there was always a bare stripe of bone between the tendon insertion and the humeral head cartilage that was narrower in the upper part of the footprint and broader toward the lower part. This bare space may be clinically relevant to correctly place implants since there is a greater risk of damaging the humeral head cartilage in the upper footprint area.

Different arthroscopic techniques to repair the SSC tendon

have been described. In the study by Richards et al. [5], one of the first on this topic, the authors described a conventional posterior portal to visualize the tendon insertion, with anterior and anterolateral portals as working portals. The technique requires the use of a 70° arthroscope to visualize the majority of the SSC insertion. Several years later, Lafosse et al. [3] described the technique of SSC repair in the beach chair position under visualization from an anterolateral portal and using anterior and anterolateral portals to insert manipulating instruments. A medial release might be needed in severely retracted cases, and the anterolateral visualization technique theoretically furnished better control of the procedure under direct visualization. While satisfactory outcomes have been reported using both techniques [19,20], the current study shows that the most critical anatomic landmarks to be considered for SSC, i.e., SSC footprint, medial long head of the biceps tendon pulley, and axillary nerve, are best visualized from the front. Based on these findings, repairing the SSC tendon using an anterolateral visualization portal is recommended.

This study has several limitations. First, the sample size was small and male and female cadavers were used due to the difficulties associated with clinical studies and obtaining specimens. Second, we did not use any digital measurement method, so the measurement accuracy could be biased. Nevertheless, we followed previously validated methods described in previous studies [11,14,16,21]. Finally, measurements were performed with the cadaver in decubitus position with the shoulder in adduction and neutral, so we consider possible modifications of these measurements with other shoulder positions used for arthroscopic SSC repair, i.e., lateral decubitus or beach chair positions. Nonetheless, Gelber et al. [22] demonstrated that the axillary nerve is closer in lateral decubitus than in the beach chair position.

Our study also has several strengths. It offers a comprehensive anatomic description of the SSC insertion, and all relevant landmarks to be considered for its repair are described in detail, such as the distance to the axillary nerve and the relationships to the biceps, the articular cartilage, and the capsule. The precise shape of the footprint and its relationships with surrounding anatomic structures are essential for correct implant placement. The relationship to the medial pulley helps improve understanding of the association between biceps instability and SSC tears. Finally, our data indicate that arthroscopic repair with an anterolateral viewing portal is preferable for repairing SSC tears.

CONCLUSIONS

Important landmarks should be considered when repairing the SSC to achieve accurate implant positioning with safer tendon release. The footprint's shape is broader proximally and tapered distally, and a clear bare stripe of bone can be identified between the tendon insertion and the humeral head cartilage. The SSC tendon insertion is closely related to the most superior part of the bicipital groove floor. At its insertion, there is also a close union of the SSC tendon to the glenohumeral capsule. We also identified a 3 cm safety zone between the lower limit of the SSC footprint and the axillary nerve. Anterior visualization might guarantee direct control of all the landmarks and allow for a safer release overall in cases of retraction.

NOTES

ORCID

Santiago Gabardo https://orcid.org/0000-0001-9242-8634
María Valencia-Mora https://orcid.org/0000-0003-0924-2930
Ismael Coifman https://orcid.org/0000-0002-6809-6008
Emilio Calvo https://orcid.org/0000-0002-6054-6078

Author contributions

Conceptualization: MVM, EC. Data curation: SG, MVM, IC. Formal analysis: SG. Methodology: MVM. Project administration: MVM. Supervision: MVM, EC. Validation: EC. Writing – original draft: SG. Writing – review & editing: SG, MVM, EC.

Conflict of interest

None.

Funding

None.

Data availability

Contact the corresponding author for data availability.

Acknowledgments

We would like to express our gratitude to Dr. Ariza for her assistance in conducting this study; Dr. Clascá for his invaluable guidance and dedication not only in this research, but in many other areas; and the entire Anatomy Department at the Autónoma de Madrid University for their support and resources, which were key in the successful completion of this project.

REFERENCES

1. Lee J, Shukla DR, Sánchez-Sotelo J. Subscapularis tears: hidden and forgotten no more. JSES Open Access 2018;2:74–83.

https://doi.org/10.5397/cise.2023.01165

2. Edwards TB, Walch G, Sirveaux F, et al. Repair of tears of the subscapularis. J Bone Joint Surg Am 2005;87:725–30.
3. Lafosse L, Lanz U, Saintmard B, Campens C. Arthroscopic repair of subscapularis tear: surgical technique and results. Orthop Traumatol Surg Res 2010;96(8 Suppl):S99–108.
4. Burkhart SS, Brady PC. Arthroscopic subscapularis repair: surgical tips and pearls A to Z. Arthroscopy 2006;22:1014–27.
5. Richards DP, Burkhart SS, Lo IK. Subscapularis tears: arthroscopic repair techniques. Orthop Clin North Am 2003;34:485–98.
6. Bell JP, Field LD. Combined intra-articular and extra-articular visualization for repair of a complete subscapularis tear: the "blended view" technique. Arthrosc Tech 2021;10:e1879–82.
7. Fox O, Lorentzos P, Farhat M, Kanawati A. The change in position of the axillary nerve with rotation of the arm. Clin Anat 2019;32:268–71.
8. Cho TH, Kwon HJ, Choi YJ, O J, Won SY, Yang HM. Intramuscular innervation of the subscapularis muscle and its clinical implication for the BoNT injection: an anatomical study using the modified Sihler's staining. Clin Anat 2019;32:110–6.
9. Burkhead WZ Jr, Scheinberg RR, Box G. Surgical anatomy of the axillary nerve. J Shoulder Elbow Surg 1992;1:31–6.
10. Clark JM, Harryman DT 2nd. Tendons, ligaments, and capsule of the rotator cuff: gross and microscopic anatomy. J Bone Joint Surg Am 1992;74:713–25.
11. Arai R, Mochizuki T, Yamaguchi K, et al. Functional anatomy of the superior glenohumeral and coracohumeral ligaments and the subscapularis tendon in view of stabilization of the long head of the biceps tendon. J Shoulder Elbow Surg 2010;19:58–64.
12. Taylor SA, Fabricant PD, Bansal M, et al. The anatomy and histology of the bicipital tunnel of the shoulder. J Shoulder Elbow Surg 2015;24:511–9.
13. Lin L, Zhang L, Cui G, Yan H. The prevalence, classification, radiological and arthroscopic findings of intratendinous subscapularis tears. Knee Surg Sports Traumatol Arthrosc 2023;31:1970–7.
14. D'Addesi LL, Anbari A, Reish MW, Brahmabhatt S, Kelly JD. The subscapularis footprint: an anatomic study of the subscapularis tendon insertion. Arthroscopy 2006;22:937–40.
15. Richards DP, Burkhart SS, Tehrany AM, Wirth MA. The subscapularis footprint: an anatomic description of its insertion site. Arthroscopy 2007;23:251–4.
16. Ide J, Tokiyoshi A, Hirose J, Mizuta H. An anatomic study of the subscapularis insertion to the humerus: the subscapularis footprint. Arthroscopy 2008;24:749–53.
17. Collin P, Matsumura N, Lädermann A, Denard PJ, Walch G. Relationship between massive chronic rotator cuff tear pattern and loss of active shoulder range of motion. J Shoulder Elbow Surg 2014;23:1195–202.
18. Curtis AS, Burbank KM, Tierney JJ, Scheller AD, Curran AR. The insertional footprint of the rotator cuff: an anatomic study. Arthroscopy 2006;22:609.
19. Saltzman BM, Collins MJ, Leroux T, et al. Arthroscopic repair of isolated subscapularis tears: a systematic review of technique-specific outcomes. Arthroscopy 2017;33:849–60.
20. Kim SJ, Jung M, Lee JH, Kim C, Chun YM. Arthroscopic repair of anterosuperior rotator cuff tears: in-continuity technique vs. disruption of subscapularis-supraspinatus tear margin: comparison of clinical outcomes and structural integrity between the two techniques. J Bone Joint Surg Am 2014;96:2056–61.
21. Kordasiewicz B, Kiciński M, Pronicki M, Malachowski K, Brzozowska M, Pomianowski S. A new look at the shoulder anterior capsuloligamentous complex complementing the insertion of the subscapularis tendon: anatomical, histological and ultrasound studies of the lesser tuberosity enthesis. Ann Anat 2016;205:45–52.
22. Gelber PE, Reina F, Caceres E, Monllau JC. A comparison of risk between the lateral decubitus and the beach-chair position when establishing an anteroinferior shoulder portal: a cadaveric study. Arthroscopy 2007;23:522–8.